D21

N79-20051

21

THE PREDICTION OF TWO-DIMENSIONAL AIRFOIL STALL PROGRESSION

Lloyd W. Gross
McDonnell Aircraft Company
McDonnell Douglas Corporation

SUMMARY

A generalized boundary condition potential flow calculation method has been combined with a momentum integral boundary layer method and a base flow theory of separation to predict airfoil viscous-inviscid interference up to and beyond stall. The resultant program considers laminar and turbulent separation and is, therefore, applicable to thin or thick airfoil stall. The calculated flow field includes the airfoil and the separation bubble recombination region behind the airfoil.

Calculated pressure distributions and equivalent airfoil shapes, including the displacement thickness of the viscous regions, are compared with flow field measurements for several airfoils. The measured displacement thicknesses and wake centerlines corroborate the calculated shape. The comparison also suggests the use of the analytical solution to evaluate the measurements.

INTRODUCTION

As part of a program for the prediction of the aerodynamic characteristics of aircraft at high angles of attack, the problem of determining the flow field around a stalled wing was addressed. A necessary preliminary step has been the development of a method of calculating the flow around a stalled two-dimensional airfoil. This capability is useful in itself, but it was developed primarily to verify the applicability of the theoretical components prior to their extension to a three dimensional calculation method.

Three types of boundary layer separation have been identified as contributing to airfoil stall. They can occur singly or in combination. The classical type of stall is due to trailing edge separation. The separating boundary layer can be either laminar or turbulent. Separation first occurs at the airfoil trailing edge and moves forward with increasing angle of attack. This type of separation leads to airfoil stall on relatively thick airfoils ($t/c > 15\% - 18\%$). Another form of separation is short bubble laminar separation where laminar separation is followed almost immediately by transition to turbulent flow and boundary layer reattachment. This bubble develops as the airfoil angle of attack is increased, or as Reynolds number is decreased, until reattachment no longer occurs. The bubble then is said to have "burst". On thick airfoils short bubble laminar separation causes a thicker downstream boundary layer, but on thinner airfoils, short bubble bursting can lead directly to airfoil stall.

When the short bubble bursts, a free shear layer is formed that recombines with the flow from the lower surface behind the airfoil trailing edge. However, under certain circumstances of airfoil thickness and Reynolds number, the flow reattaches to the airfoil surface and a new turbulent boundary layer is formed. This is referred to as a long laminar separation bubble. Increases of angle of attack cause the bubble length to increase until reattachment moves behind the airfoil trailing edge.

The present analytical description of airfoil stall progression is based upon a potential flow calculation method that allows either the airfoil shape or pressure distribution to be used as the boundary condition over any portion of the airfoil surface. This potential flow calculation method is combined with momentum integral boundary layer calculation methods and a component analysis description of separated base flow to form a unified viscous-inviscid interaction theory. The three types of separated flow mentioned above are included whether they occur singly or in combination.

NOMENCLATURE

c	airfoil chord
C_p	pressure coefficient
t	airfoil thickness
U	velocity on airfoil surface
U_∞	freestream velocity
x	horizontal distance
α	angle of attack

MATHEMATICAL MODEL

The viscous-inviscid interaction around an airfoil with separation is modeled by finding the equivalent displacement surface of the viscous flow around the airfoil and into the wake. Paneling is laid out on the chord line of the airfoil and is extended beyond the trailing edge to include the wake. An inviscid calculation is made as the initial step of an iterative procedure. A boundary layer calculation method is used to determine the displacement thickness of the attached viscous flow and the point of separation. The displacement thickness is added to the basic airfoil to form the equivalent airfoil shape. Downstream of separation, the displacement thickness is not known, so the pressure predicted by a base flow theory is used as the boundary condition. The output of this calculation is an updated pressure distribution and equivalent airfoil shape. The updated pressure distribution then is used as the

input for improved viscous flow calculations. This procedure is repeated until the pressure distribution of the equivalent airfoil is compatible with the pressure rises predicted by the viscous theories. The analytical methods that were used are described in detail in Reference 1. However, the potential flow calculation method and the method of modeling the separated flow region will be described because of their importance to the method.

Potential Flow Calculation

Bristow (Reference 2) recognized that when the boundary conditions of a chord-line singularity potential flow calculation method are linearized in the region of the body surface, the boundary condition for each singularity can be interchanged between the surface slope and the tangential flow velocity at the panel control point. The resulting Generalized Boundary Condition method allows the geometry to be specified for areas where the viscous flow is attached to the body and the velocity or pressure to be specified for areas with separated flow or in the wake. This approach is illustrated in Figure 1. It was recognized that a chord-line singularity method is less accurate than a surface singularity method. However, a generalized boundary condition surface singularity method is still in development (Reference 3) and it was felt to be desirable to develop the methodology of the viscous solution in the meantime.

Separation Bubble Model

The model for a separation bubble was taken from the component analysis base flow theory developed by Chapman, Korst and Chow (e.g., Reference 4). This theory assumes a turbulent shear layer between the outer potential flow and the inner recirculating flow (Figure 2). Then, with the argument that the momentum within the shear layer originates in the outer flow, a streamline is identified such that the momentum of the total shear layer is contained within the equivalent inviscid flow between this streamline and the outer edge of the shear layer. If this is the limiting streamline between the inner and outer flows, the momentum balance of the outer flow is assured. The velocity of the limiting streamline determines the pressure rise across the separation bubble since it approaches its stagnation pressure at the point of reattachment or recombination with the shear layer from the lower surface. Initially, the pressure within the bubble is constant. Then, at some point within the bubble (near the airfoil trailing edge for a trailing edge bubble), the pressure starts to increase toward the pressure at reattachment or recombination. It is from this recompression region that mass is pumped into the forward part of the bubble in order to set up the circulation within the bubble.

Application of the base flow theory to describe trailing edge separation is shown in Figure 2. In this case the shear layer from the upper surface combines with the shear layer from the lower surface and forms a wake. The same physical picture is assumed to occur in the leading edge separation bubbles except that the shear layer intersects the airfoil surface. At this point a new turbulent boundary layer is formed which continues downstream.

From this physical picture, it can be seen that the pressure within the separation bubble is limited by the static pressure at the closure of the bubble and not by the pressure at separation. A solution to the flow problem is reached when the presence of the separation bubble modifies the pressure distribution around the airfoil sufficiently that the pressure at separation agrees with the bubble pressure.

VERIFICATION OF THE METHOD

The Generalized Boundary Condition potential flow calculation method and the separation bubble model were combined with momentum integral boundary layer methods into a procedure for calculating the viscous-inviscid interactions for a wide range of airfoils. The resulting program is self-contained and includes all of the logic for distinguishing between the types or combinations of separated flow that are present. An iterative procedure is used to go from the initial inviscid solution to the viscous solution. In addition, iterative sub-loops are required to determine the proper bubble pressures for the long laminar separation bubble and the trailing edge bubble. The iteration procedure is described in Reference 1.

In order to test the ability of this analytical model to predict the flow field around an airfoil with various types of separated flow present, five airfoils of different thickness ratios were studied. The experimental data for these airfoils were taken from References 5 and 6. They were: (1) the 63_3-018 airfoil with stall development by progression of turbulent separation from the trailing edge forward, (2) the 63_1-012 airfoil which stalled by the sudden bursting of a short separation bubble, (3) the 63-009 airfoil that also stalled by short bubble bursting, (4) the 64A-006 airfoil with stall development by the progressive growth of a long separation bubble until its reattachment point moved past the airfoil trailing edge, and (5) the GA(W)-1 airfoil which stalled similarly to the 63_3-018 airfoil but represented more advanced airfoil design. The calculations were made for the specific angles of attack at which the surface pressures on the model had been measured.

Representative calculated pressure distributions and equivalent airfoil surfaces are shown in Figures 3 and 4. The inviscid pressure distribution is shown for comparison with the calculated pressure distribution and the measured pressures. The equivalent airfoil shape is the combination of the airfoil and the displacement surface of the viscous flow. The limiting streamline between the continuing viscous flow and the recirculating bubble flow also is shown.

Figure 3 shows a thin airfoil with a long laminar separation bubble. In order to simulate this flow, it was necessary to assume a bubble pressure and a point of reattachment. The pressure distribution was prescribed between separation and reattachment, and the airfoil shape was prescribed outside of this region. The subsequent equivalent airfoil shape was determined by the Generalized Boundary Condition program and the shape of the limiting streamline from the base flow theory. Reattachment was defined as the point where the limiting streamline intersected the airfoil surface. If the pressure rise between separation and reattachment corresponded to the predictions of the

base flow theory, then the solution was complete. Otherwise a higher bubble pressure was assumed, and the assumed reattachment point was updated by the results of the previous calculation.

The predicted bubble pressures shown in Figure 3 are somewhat lower than experiment and there is a kink in the pressure distribution at reattachment. The first effect is due to the inherent limitations of the chordline singularity potential flow calculation method. The second is due to the use of finite paneling. Also shown in Figure 3 are displacement thicknesses calculated from the measured boundary layer velocity profiles of Reference 5. These compare closely with the calculated equivalent airfoil surface, indicating that the shear layer growth across the separation bubble is calculated properly.

Figure 4 shows the calculated results for the NACA 63_1-012 airfoil at an angle of attack that is sufficiently high that short laminar separation bubble bursting has occurred. This figure is a good illustration of the fact that the equivalent airfoil contour terminates in an open wake. The method therefore has the potential for calculating the drag of the airfoil as well as the lift and pitching moment. This was not done since the present method is not considered to be sufficiently accurate for such a sensitive parameter. However, the method using a surface singularity potential flow method should be capable of this calculation.

The equivalent airfoil surfaces of the NASA GA(W)-1 airfoil were calculated at three angles of attack and are shown in Figures 5, 6, and 7 superimposed on the flow field measurements of Seetharam and Wentz (ref. 6). The measured boundary layer displacement thickness and wake centerlines also are shown. It was the object of this effort to try to develop some insight on just how the bubble matched the pressure isobars. This should be of importance for the development of a surface singularity method. It should have the further advantage of allowing an evaluation of the measured flow field; in particular, it should give an appreciation of the effect of the wind tunnel walls.

Figure 5 shows the wing at an angle of attack $\alpha = 10.3°$. A true separation bubble has not yet formed as evidenced by the pressure recovery all the way to the trailing edge. However, there is some recirculating flow just aft of the trailing edge. The measured displacement thickness agrees reasonably well with the equivalent airfoil surface as does the wake centerline. The calculated wake is much thicker than the measured wake indicating that the calculations did not allow sufficient pressure rise in the wake.

At an angle of attack $\alpha = 14.4°$, a full separation bubble has formed (Figure 6). In this case, the measured displacement thickness does not agree with the calculated equivalent airfoil surface, although the measured wake centerline does. It is noted that the measured displacement thicknesses do not agree with the measured separation point. This is stated to occur at the point of largest pressure gradient on the airfoil surface while a projection of the displacement thicknesses to the airfoil surface indicates later separation. Measured and calculated separation points agreed within 2% of the airfoil chord.

A fully developed trailing edge separation bubble at an angle of attack $\alpha = 18.4°$ is shown as Figure 7. Of particular note is the constant pressure region that brackets the equivalent airfoil contour. The measured displacement thickness also agrees with the calculated contour. However, there is a marked deviation of the measured wake centerline. This is probably due to the effects of the wind tunnel floor and ceiling which are known to have a pronounced effect on the airfoil downwash when separated flow is present.

These results suggest an approach to the determination of wind tunnel wall corrections for separated flows. Potential flow calculation methods have been developed to simulate the flow around airfoils between parallel walls. The addition of singularity panels simulating such parallel walls in the current program should lead to closer agreement with the measured flow shown in Figure 7. The difference between the two cases would yield both streamline curvature and blockage corrections.

CONCLUDING REMARKS

The McDonnell Aircraft Company Generalized Boundary Condition potential flow calculation method has been combined with momentum integral boundary layer methods and a component analysis base flow theory to develop a method for predicting viscous-inviscid interacting flows on airfoils beyond the appearance of boundary layer separation. The physical models of the several phases of such flows have been identified and combined into a functioning whole that accounts for the interaction of attached flow, short and long leading edge separation bubbles, and trailing edge bubbles. The resultant computer program has been used to calculate the pressure distribution and equivalent airfoil shape for airfoils exhibiting the different types of separated flow. It also has been used to evaluate flow field measurements around an airfoil with trailing edge separation.

REFERENCES

1. Gross, L. W., "The Prediction of Two-Dimensional Airfoil Stall Progression," AIAA Paper 78-155, January 1978.

2. Bristow, D. R., "Computer Program to Solve the Three-Dimensional Mixed Boundary Condition Problem for Subsonic or Supersonic Potential Flow," McDonnell Douglas Corporation Report A3190, December 1974.

3. Bristow, D. R., "Recent Improvements in Surface Singularity Methods for the Flow Field Analysis about Two-Dimensional Airfoils," AIAA Paper 77-541, June 1977.

4. Korst, H. H., "A Theory for Base Pressures in Transonic and Supersonic Flow," Journal of Applied Mechanics, Vol. 23, Transactions ASME, Vol. 78, 1956, pp. 593-600.

5. McCullough, G. B. and Gault, D. E., "Examples of Three Representative Types of Airfoil-Section Stall at Low Speed," NACA TN 2502, July 1951.

6. Seetharam, H. C. and Wentz, W. H. Jr., "Experimental Studies of Flow Separation and Stalling on a Two-Dimensional Airfoil at Low Speeds," NASA CR-2560, July 1975.

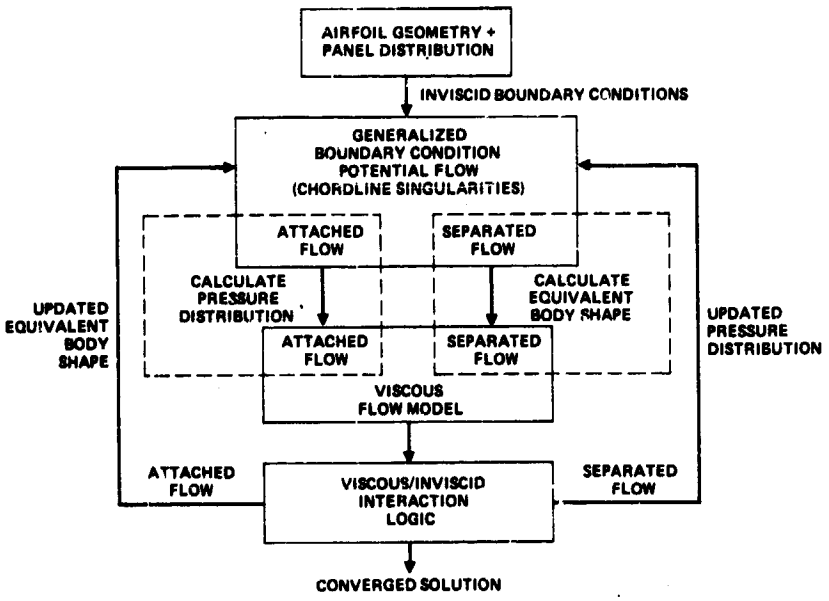

Figure 1.- Applications of generalized boundary conditions to separated flow modeling.

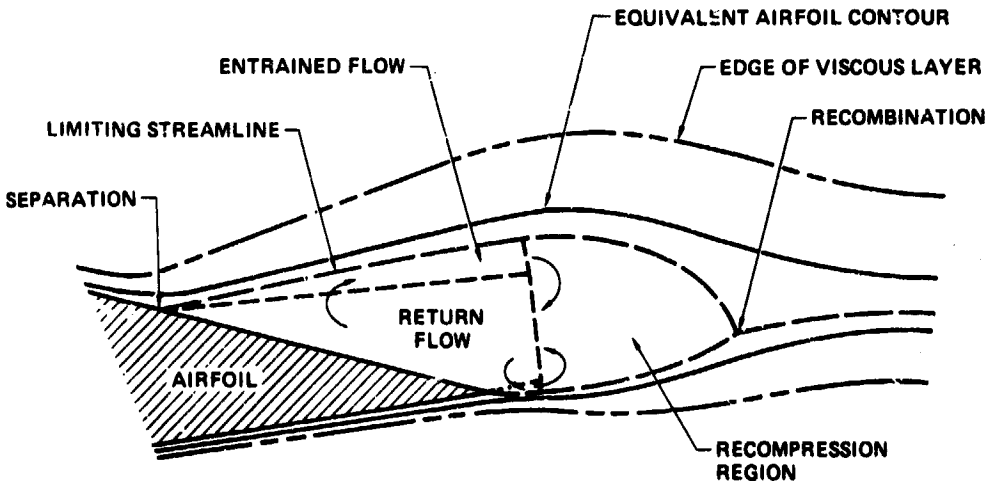

Figure 2.- Model of boundary-layer separation bubble developed from the component-analysis base-flow theory.

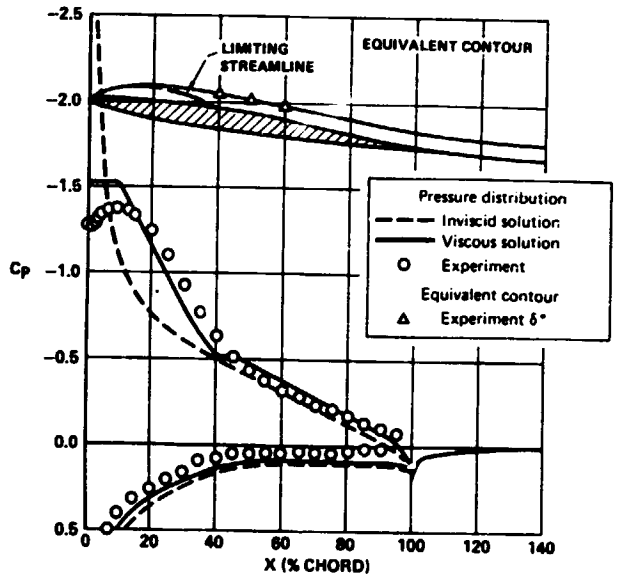

Figure 3.- Prediction of airfoil pressure distribution and equivalent contour 64A-006 airfoil. $\alpha = 7.31°$.

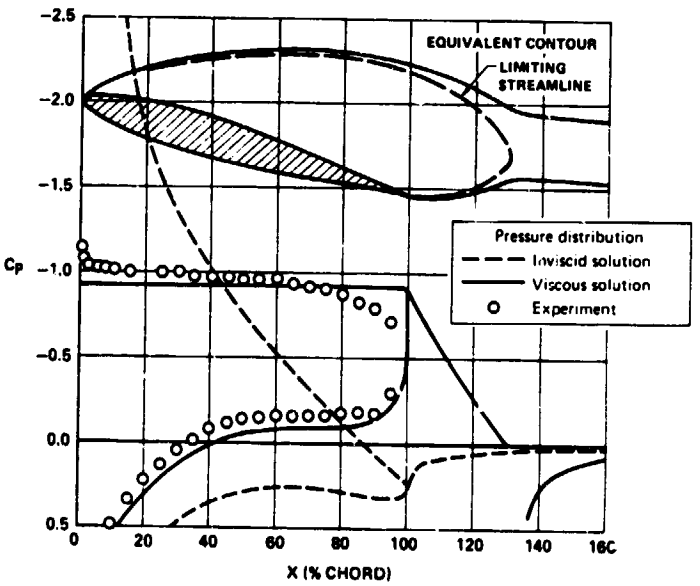

Figure 4.- Prediction of airfoil pressure distribution and equivalent contour 63_1-012 airfoil. $\alpha = 15.01°$.

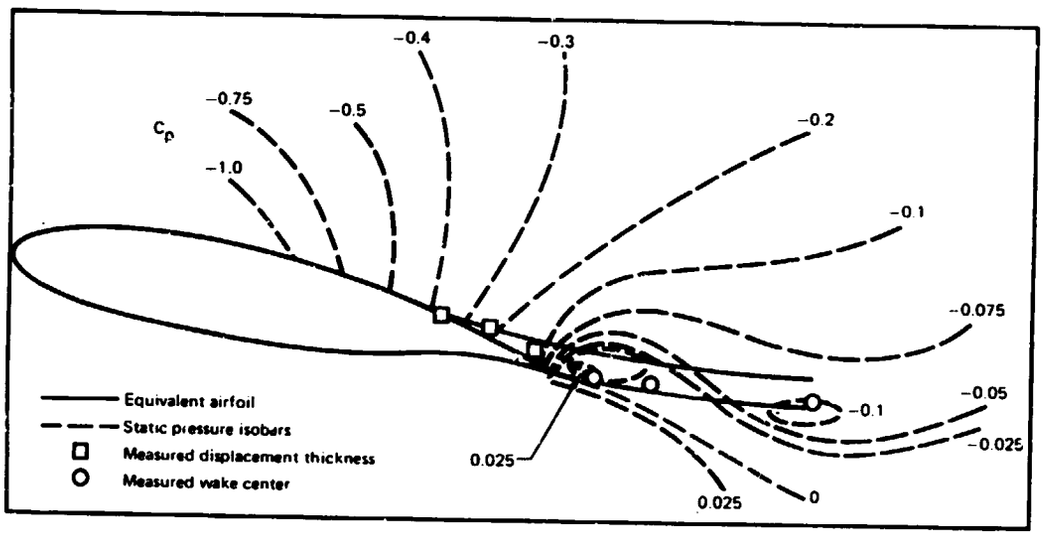

Figure 5.- Superposition of calculated equivalent airfoil shape on measured flow field of GA(W)-1 airfoil at $\alpha = 10.3^{o}$.

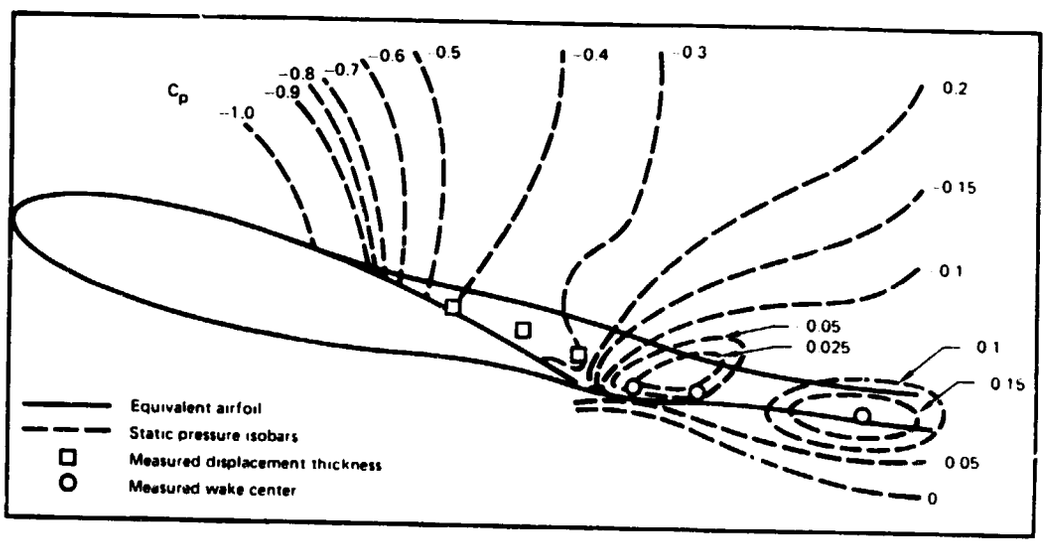

Figure 6.- Superposition of calculated equivalent airfoil shape on measured flow field of GA(W)-1 airfoil at $\alpha = 14.4°$.

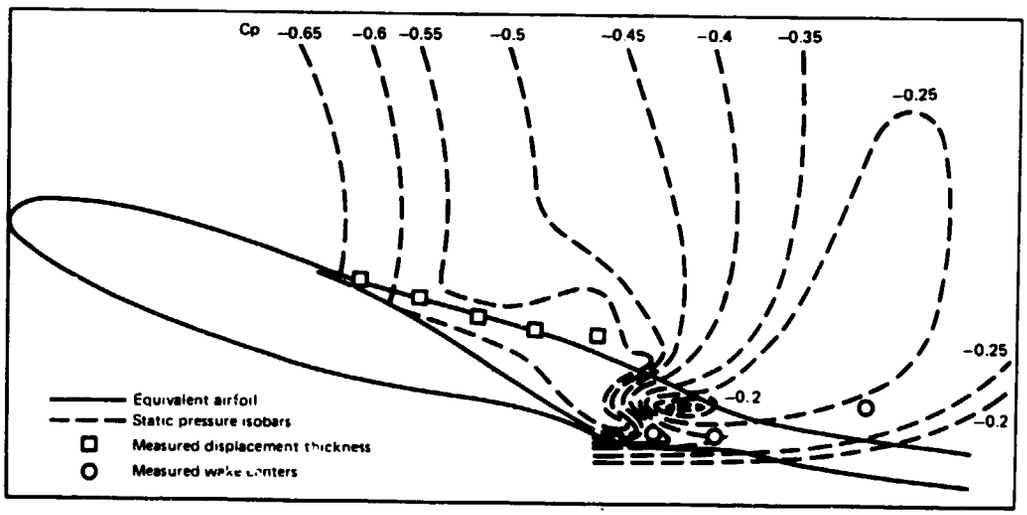

Figure 7.- Superposition of calculated equivalent airfoil shape on measured flow field of GA(W)-1 airfoil at $\alpha = 18.4°$.